New metastatic model of human small-cell lung cancer by orthotopic transplantation in mice

Shuichi Sakamoto, Hiroyuki Inoue, Shunichi Ohba, Yasuko Kohda, Ihomi Usami, Tohru Masuda, Manabu Kawada and Akio Nomoto

Institute of Microbial Chemistry, Numazu, Japan

Small-cell lung cancer (SCLC) is an aggressive cancer with high metastatic ability and novel strategies against the metastasis are urgently needed to improve SCLC treatment. However, the mechanism of metastasis of SCLC remains largely to be elucidated. For further studies of SCLC metastasis, we developed a new orthotopic transplantation model in mice. We established a GFP-labeled subline from the human SCLC cell line DMS273 and transplanted them orthotopically into the lung of nude mice with Matrigel. The GFP-labeled cells showed significant metastatic activity and formed metastatic foci in distant tissues such as bone, kidney, and brain, as observed in SCLC patients. From a bone metastasis focus of the mouse, we isolated another subline, termed G3H, with enhanced metastatic potential and higher hepatocyte growth factor (HGF) expression than the parental line. Further studies indicated that the HGF/MET signaling pathway was involved in *in vitro* motility and invasion activities of the G3H cells and treatments with MET inhibitors decreased formation of distant metastases in our orthotopic model using G3H cells. These data indicated that our model mimics the clinical aspect of SCLC such as metastatic tropism and autocrine of HGF/MET signaling. Compared with other orthotopic SCLC models, our model has a superior ability to form distant metastases. Therefore, our model will provide a valuable tool for the study of SCLC metastasis.

Small-cell lung cancer (SCLC) accounts for 10–20% of lung cancer cases and is found almost exclusively in smokers.[1] Small-cell lung cancer is histologically distinct from all other forms of lung cancer, collectively known as non-small-cell lung cancer,[2] and can be classified into two subtypes based on histological features and gene expression profile: classic (approximately 70% of total SCLC) or variant (approximately 30%).[3,4] The abilities to develop resistance against chemotherapies and to form early and widespread metastases are responsible for the high malignancy of SCLC. As a result, the overall survival of SCLC at 5 years has been 5–10% over the last several decades.[5] Hence, development of novel strategies against SCLC, especially targeting metastasis, is urgently needed.

The receptor tyrosine kinase MET is the receptor for HGF, and activation of the HGF/MET signal is involved in cell proliferation, survival, and motility.[6] Constitutive activation of this signal is often observed in many tumors. In SCLC patients, mutation of MET,[7] elevation of serum HGF levels,[8,9] autocrine/paracrine regulation of HGF/MET signal,[10] and association of MET phosphorylation with worse prognosis[11] have been reported. Moreover, an *in vitro* study showed that motility of SCLC cells was enhanced by ligand stimulation with HGF through MET.[12] Together this indicates that the HGF/MET signal plays important roles in SCLC biology.

Although significant roles of the HGF/MET signal in SCLC have been observed, understanding the molecular mechanism of metastasis of SCLC, which is important for the development of an effective treatment, remains to be elucidated. Tumor metastasis is a complex phenomenon and consists of many steps that involve interactions of tumor cells with the microenvironment in the primary tumor tissues and metastatic foci.[13] Xenograft models constructed by orthotopic transplantation of human tumor cells into immunodeficient mice have been recognized as useful tools for the study of metastasis, because orthotopic transplantation can mimic the original primary tumor microenvironment.[14,15]

Here, we found that GFP-labelled sublines of the human SCLC cell line DMS273 had significant metastatic activity when the cells were orthotopically implanted. Using these cells, we successfully developed a new orthotopic transplantation model of SCLC metastasis and examined the role of the HGF/MET signal in our model.

Materials and Methods

Animal experiments. Female BALB/c nude mice, 5 weeks old, were obtained from Charles River Japan (Kanagawa, Japan). Mice aged 8 weeks were used for the *in vivo* metastasis assay. A total of 1.33×10^8 GFP-labelled DMS273 cells (DMS273-GFP or G3H cells) were suspended in 0.8 mL BD Matrigel Growth Factor Reduced (Becton, Dickinson & Company, Tokyo, Japan):DMEM (5:3) solution. Before injection, mice were anesthetized with pentobarbital and a 1.5-cm-long incision was made in the skin on their left side. A total of 20 μL suspension (containing 1×10^6

Original Article
New orthotopic model for SCLC metastasis
www.wileyonlinelibrary.com/journal/cas

Table 1. Orthotopic tumor growth and metastasis of DMS273-GFP and G3H cells in nude mice

Cells	Orthotopic tumor formation, n (%)	Tumor volume, mm^3	Metastasis incidence, n (%)	Location of metastasis						Survival, days
				Bone	Brain	Lymph node	Kidney	Adrenal gland	Liver	
DMS273-GFP										
Exp. 1 (n = 11)	11 (100)	375 ± 199	5 (45)	2	2	3	2	0	1	41.5 ± 11
Exp. 2 (n = 9)	9 (100)	446 ± 180	4 (44)	2	0	2	0	0	1	33.6 ± 4.1
G3H										
Exp. 1 (n = 11)	10 (91)	357 ± 254	7 (64)	3	3	2	2	1	0	39.9 ± 9.6
Exp. 2 (n = 11)	11 (100)	269 ± 111	7 (64)	3	5	0	1	0	0	32.8 ± 3.9

Cells (1×10^6) were injected into the left lung of nude mice. Mice were killed when they became moribund, and orthotopic and metastatic tumor formations were assessed by GFP fluorescence. Exp., experiment.
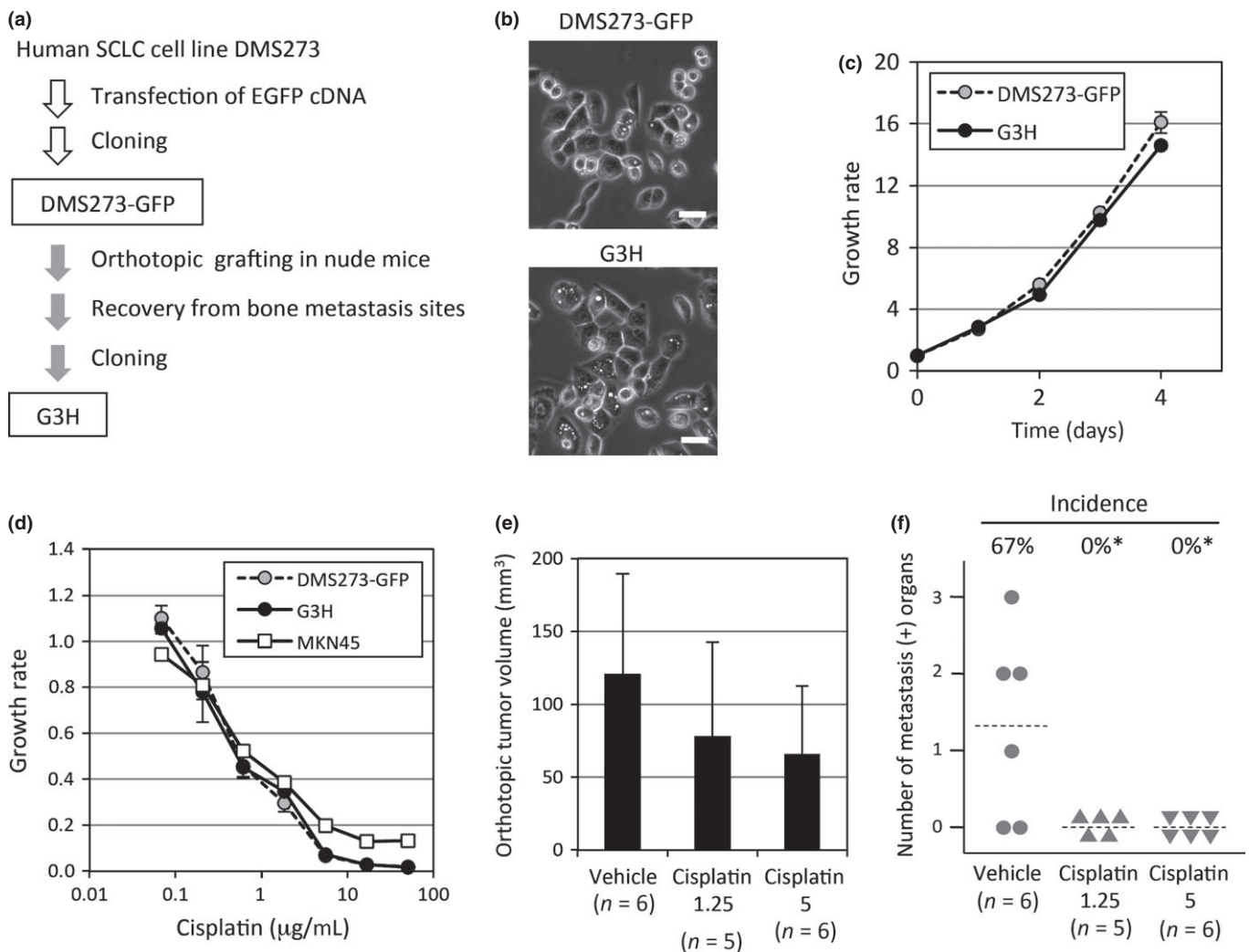

Fig. 1. Green fluorescent protein-labelled metastatic sublines of human small-cell lung carcinoma (SCLC) cell line DMS273 and effect of cisplatin treatment. (a) Establishment of GFP-labelled metastatic sublines of DMS273. (b) Cell morphology of DMS273-GFP and G3H cells. Bar = 50 μm. (c) *In vitro* growth rate of the DMS273 sublines as determined by MTT assay. The growth rate was calculated as the ratio of the absorbance from cultured cells compared with that of day 0. Values are expressed as means of triplicate experiments ± SD. (d) *In vitro* sensitivity of the DMS273 sublines and MKN45 cell line against cisplatin. Cells were treated in triplicate with the indicated concentrations of cisplatin for 72 h. The growth rate was calculated as the ratio of MTT absorbance from cisplatin-treated cells compared with that of untreated cells. Results are expressed as means ± SD from three independent experiments. (e, f) Effect of cisplatin treatment on orthotopic and metastatic tumor formation in our model using G3H cells. The mice were killed and assessed on day 25 or 26. (e) Orthotopic tumor formation. Results are expressed as means ± SD (n = 5–6). (f) Distant metastatic tumor formation. The dotted lines show the means of the number of metastasis-positive organs of each group. Percentages show distant metastases incidence. *$P < 0.05$, Fisher's exact test.

cells) was injected into the left lung of nude mice using a 30-gauge needle between the third and fourth ribs. The wound was then blocked up with surgical clips. After the indicated periods, the mice were killed and the Olympus OV110 Small Animal Imaging System (Olympus Corp., Tokyo, Japan) was used for imaging orthotopic and

metastatic tumor formations. The length (L) and width (W) of the orthotopic tumor measured by calipers and the tumor volume (TV) was calculated using the formula: TV = ($L \times W^2$)/2.

Statistical analysis. Results are presented as mean ± SD. Significance of the differences between means was assessed using Student's *t*-test for *in vitro* experiments and orthotopic tumor formation, and using Fisher's exact test for distant metastatic formation. Differences were considered statistically significant at $P < 0.05$.

Other methods. Cell lines, reagents, conditioned medium (CM), *in vitro* growth rates/chemosensitivity, *in vitro* motility /invasion assay, real-time PCR analysis, Western blot analysis, cytokine array analysis and ELISA, drug treatments for animals, and histopathological study are described in Document S1.

Results

Development of a new orthotopic SCLC metastasis model. We previously implanted a GFP-labelled subline of the human variant SCLC cell line DMS273 (DMS273-GFP cells) orthotop-ically into the left lung of nude mice and found that the cells showed significant metastatic activity (data not shown). This finding led us to develop a new orthotopic SCLC metastasis model using these cells. After preliminary examinations under various conditions, we found that after inoculation of 1×10^6 cells of DMS273-GFP suspended with Matrigel, over 90% of the inoculated animals developed tumors at the injected site and over 40% showed metastases after 20–40 days of injection (Table 1). The metastatic organs of the cells were similar to SCLC patients, and included bone, brain, and lymph node (Table 1). To obtain highly metastatic variants, we recovered the tumor cells from a bone metastasis of our model, cultured the cells *in vitro* and cloned several sublines (Fig. 1a). One of the sublines, termed G3H, showed enhanced metastatic activity (>60% of inoculated animals had metastases) with nearly the same metastatic tropism of the parental line (Fig. 2a–j, Table 1). Using immunohistological analysis, we confirmed that the cells in the formed tumor at the orthotopic transplantation site and the distant metastatic sites were GFP-positive (Fig. 2k–v), and that a large part of the cells in the orthotopic site and the bone metastatic site were Ki67-positive (Fig. S1a,
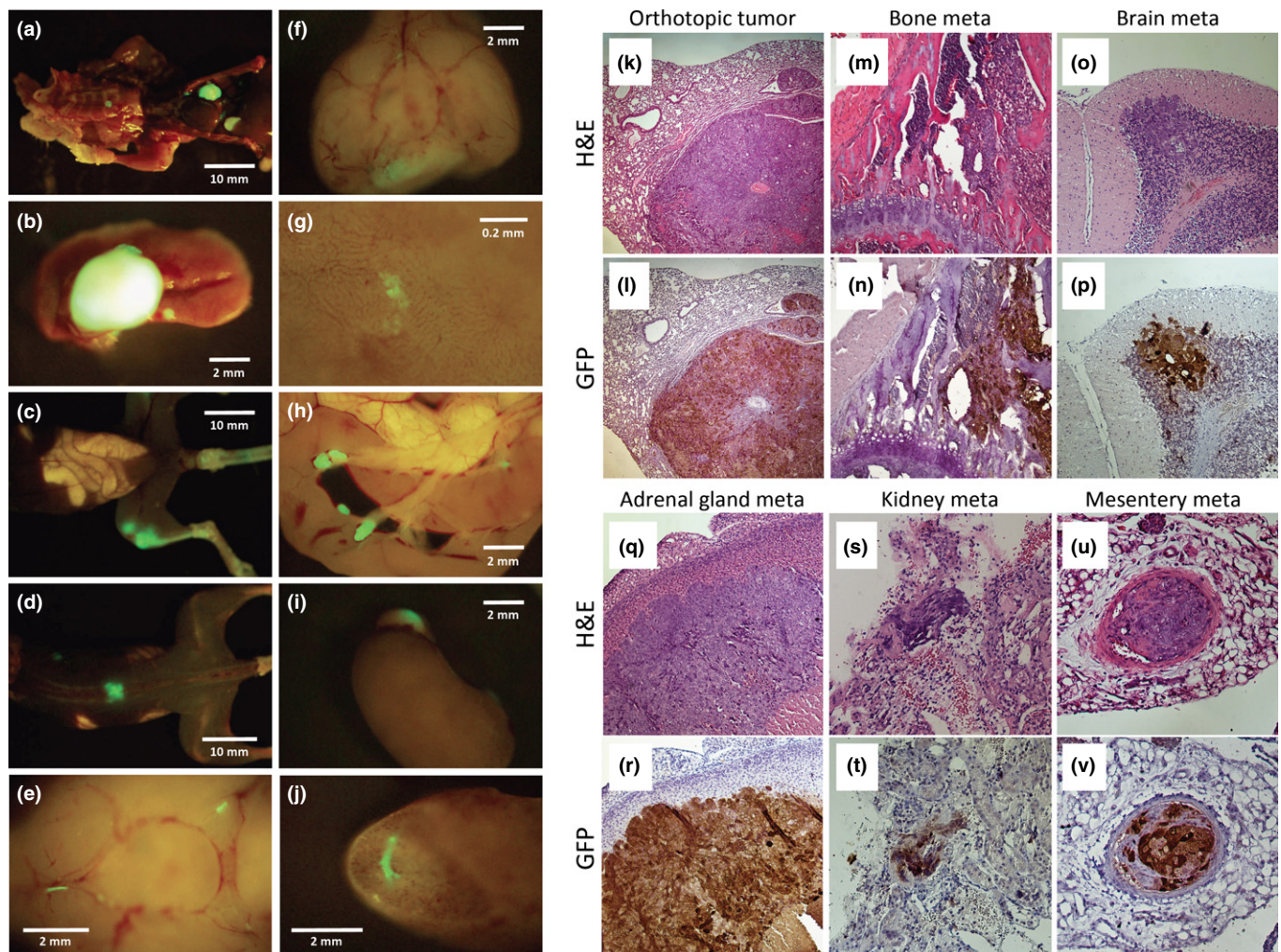

Fig. 2. Orthotopic and metastatic tumor formation of G3H, a GFP-labelled subline of human small-cell lung carcinoma cell line DMS273, in nude mice. Intrapulmonary injected cells formed tumor at the injected site of lung and metastatic colonies in various distant organs. (a–j) Representative GFP fluorescent images of orthotopic and metastatic tumor formation of G3H cells in lung (a, b), femur (c), vertebra (d), brain (e, f), liver (g), mesentery lymph node (h), adrenal gland (i), and kidney (j). (k–v) Representative histological appearance of orthotopic tumors (k, l) and metastatic (Meta) tumors in bone (m, n), brain (o, p), adrenal gland (q, r), kidney (s, t), and a blood vessel of mesentery (u, v). (k, m, o, q, s, u) H&E staining; (l, n, p, r, t, v) GFP immunostaining. Magnification, ×40 (k, l), ×100 (m–r), ×200 (s–v).

Original Article
New orthotopic model for SCLC metastasis
www.wileyonlinelibrary.com/journal/cas

b). We also detected expression of the neuroendocrine marker secretogranin II, which is often observed in SCLC, in the orthotopic tumor (Fig. S1c,d). In addition, we analyzed the differences in angiogenesis (CD31), lymphangiogenesis (LYVE1), and stromal reaction (αSMA) between the orthotopic tumors of DMS273-GFP and G3H cells, but we did not observed any significant differences (Fig. S2). These findings showed that the GFP-labelled subline of DMS273 exhibited the potential to form both orthotopic primary tumor and metastasis to distant organs in nude mice.

Next we investigated the *in vitro* characteristics of the DMS273-GFP parental line and highly metastatic subline G3H. Phase-contrast microscopy revealed that G3H cells had similar morphology to the parental DMS273-GFP cells (Fig. 1b). No significant differences were observed in *in vitro* cell growth rates between G3H and parental DMS273-GFP cells (Fig. 1c) or in *in vitro* motility and invasion assays using Transwell chambers (data not shown).

Effect of cisplatin treatment in orthotopic model of SCLC metastasis. We next tested the antitumor effect of cisplatin, which is used as first-line treatment for SCLC.[1] *In vitro* cytotoxic assays showed that both G3H and parental DMS273-GFP

cells had cisplatin sensitivity similar to the human gastric cancer cell line MKN45, and their IC_{50} values were approximately 0.5 μg/mL in 72-h treatment experiments (Fig. 1d). This result is consistent with previous data showing that both DMS273 and MKN45 exhibited an average sensitivity to cisplatin in the JFCR39 cancer cell line panel.[16]

We next carried out *in vivo* orthotopic experiments and treated mice with cisplatin at doses of 1.25 or 5 mg/kg once a week. Compared with the vehicle-treated group, mice treated with 1.25 or 5 mg/kg cisplatin had 35% and 45% reduction in orthotopic tumor formation, respectively (not statistically significant) (Fig. 1e). Interestingly, distant metastatic formation in our model was significantly decreased with cisplatin treatment at both doses ($P < 0.05$) (Fig. 1f). These results suggest that our model was useful for the assessment of antimetastatic efficacy of antitumor compounds.

Higher expression of HGF in metastatic subline G3H. Tumor cells secrete cytokines that affect tumor growth and metastasis. Thus, we carried out an analysis of the CM of DMS273-GFP and G3H cells using a human cytokine antibody array. Both cell lines produced interleukin-8, monocyte chemotactic protein-1, granulocyte/macrophage colony-stimulating fac-
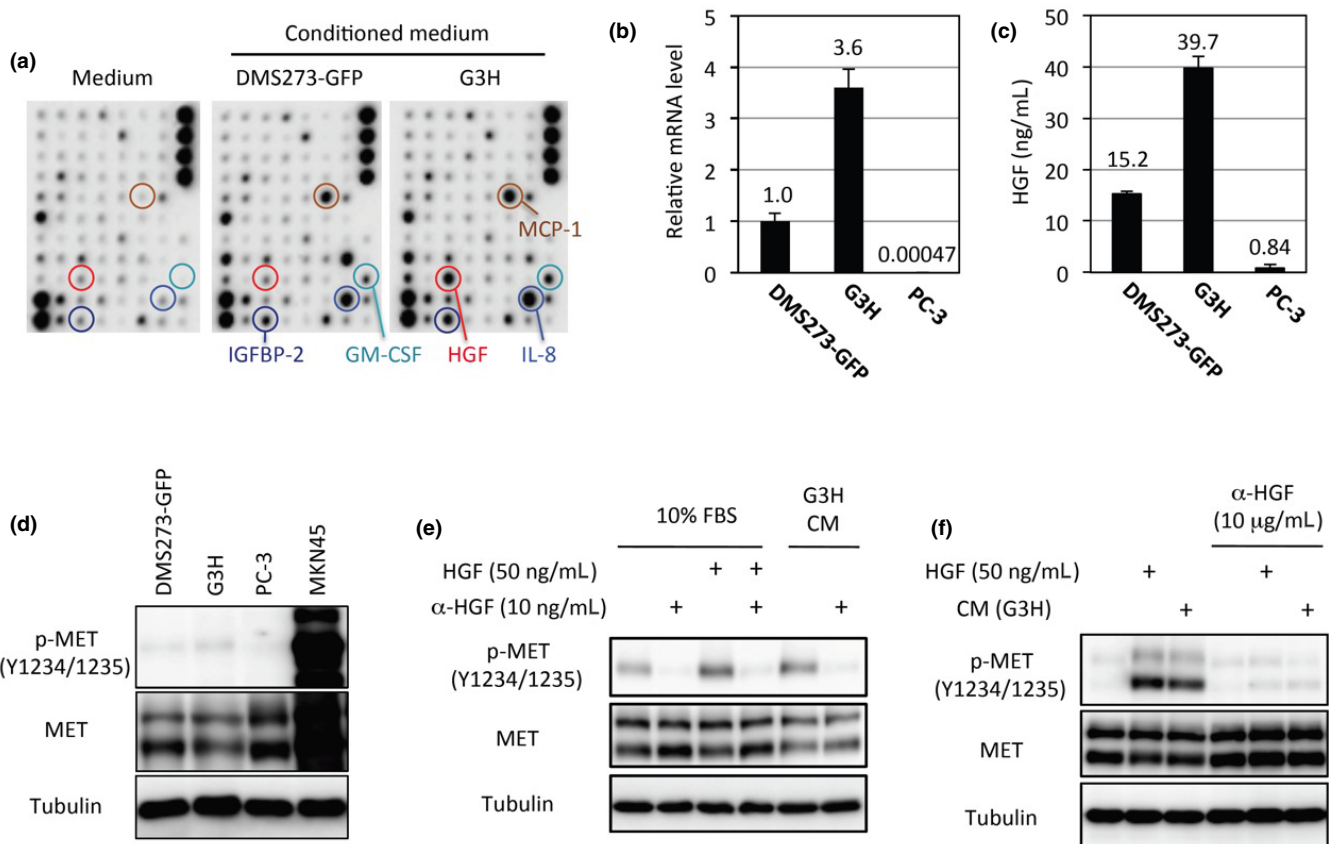

Fig. 3. Hepatocyte growth factor (HGF)/MET signal in the metastatic sublines of small-cell lung carcinoma cell line DMS273. (a) Images of Ray-Bio C-Series Human Cytokine Antibody Array 5 that were incubated with conditioned media (CM) or control media. The HGF, granulocyte/macrophage colony-stimulating factor (GM-CSF), insulin-like growth factor-binding protein-2 (IGFBP-2), interleukin-8 (IL-8), and monocyte chemotactic protein-1 (MCP-1) signals are marked with circles. (b) Quantitative analysis of HGF mRNA. Total RNA (1 μg) extracted from subconfluent cells were subjected to real-time RT-PCR. Results are expressed as means of three independent experiments ± SD. (c) ELISA of HGF protein in CM. Cells were incubated with DMEM containing 10% FBS for 3 days and the CM was harvested. Results are expressed as means of three independent experiments ± SD. (d) Western blot analysis for MET. Whole cell lysate (20 μg) was separated on a 7.5% SDS-PAGE and membranes were blotted with anti-phosphorylated MET (pY1234/1235) (top panel), anti-MET (second panel), or α-tubulin (bottom panel, loading control). (e, f) Effect of anti-HGF neutralizing antibodies on MET phosphorylation induced by CM of G3H. G3H (e) or PC-3 (f) cells were starved in DMEM containing 0.5% FBS overnight and pre-incubated with anti-HGF neutralizing antibody (10 μg/mL) for 2 h. Cells were then incubated with CM of G3H or recombinant HGF (50 ng/mL) for 15 min. Cells were lysed immediately and whole cell lysate (20 μg) was analyzed by Western blotting.

tor, insulin-like growth factor-binding protein-2, and HGF (Fig. 3a). Interestingly, real-time RT-PCR analysis and ELISA revealed that G3H showed higher expressions of both HGF mRNA and protein than DMS273-GFP cells (Fig. 3b,c), indicating that the bone metastasis-derived G3H cells have an increased HGF expression level compared with the parental line.

Hepatocyte growth factor/MET signal in metastatic subline G3H. As the HGF/MET signal is involved in cellular motility and invasion in various cancers including SCLC,[6,12] we further evaluated the HGF/MET signal in G3H cells. MET protein, a natural receptor for HGF, was detected in both DMS273-GFP and G3H cells by immunoblot analysis (Fig. 3d). MET protein levels in DMS273-GFP and G3H cells were significantly lower than that in prostate cancer PC-3 cells. MET is activated by binding with its ligand HGF at the cell surface, upon which MET is autophosphorylated on its intracellular domain. In normal culture conditions (DMEM containing 10% FBS), a certain basal MET phosphorylation (at the autophosphorylation sites Tyr1234/1235) was observed in G3H cells (Fig. 3e). Treatment of G3H cells with recombinant human HGF in 10% FBS medium significantly induced autophosphorylation of MET (Fig. 3e). Both basal level and recombinant HGF-induced MET phosphorylation disappeared after treatment with anti-HGF neutralizing antibody (Fig. 3e). These results indicated that MET is functional in G3H cells, and that cells are sensitive to HGF.

Next, we determined whether HGF secreted from G3H cells was functional. Treatment with CM of G3H cells induced slightly higher levels of MET phosphorylation in G3H cells compared with 10% FBS, and this induction was cancelled by treatment with anti-HGF neutralizing antibody (Fig. 3e). We also found that the MET protein level was higher (Fig. 3d) and HGF was remarkably lower in human prostate cancer PC-3 cells compared with G3H cells (Fig. 3b,c). In PC-3 cells, basal MET phosphorylation in medium containing 10% FBS was very low, and both recombinant human HGF and CM of G3H cells strikingly induced MET phosphorylation (Fig. 3f). These inductions of MET phosphorylation in PC-3 cells were cancelled by treatment with anti-HGF neutralizing antibody as in G3H cells (Fig. 3f). These results indicated that G3H cells express functionally active HGF and MET, and suggested the existence of an autocrine activation of the HGF/MET signal in G3H cells.

Pharmacological evaluation of the role of HGF/MET inhibitor signal in the model. The above data prompted us to examine the effect of a highly specific MET inhibitor PHA665752[11,17] in our model, *in vitro* exposure of 0.2 μM PHA665752 completely inhibited both basal and HGF-induced MET phosphorylation in G3H cells (Fig. 4a), indicating that PHA665752 is a potent inhibitor of MET in the cells. Both G3H and DMS273-GFP cells showed similar sensitivities to PHA665752 and their IC_{50} values were approximately 2 μM in 72-h treatment experiments (Fig. 4b). In contrast, the gastric cancer cell line MKN45, which harbors *MET* gene amplification and is MET-addicted,[18] showed a severe sensitivity to PHA665752 with IC_{50} values of approximately 50 nM (Fig. 4b). As expected, the immunoblot experiments showed that MKN45 had extremely higher expression levels of phosphorylated MET (pY1234/Y1235) and total MET protein than DMS273-GFP,
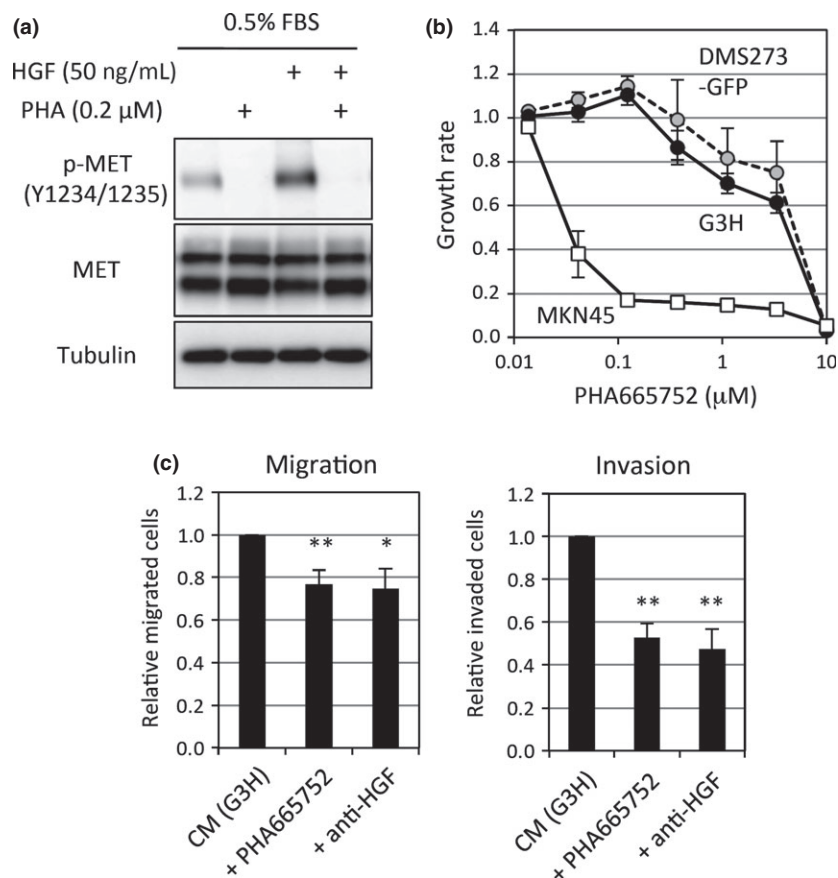
Fig. 4. *In vitro* effect of PHA665752, a small molecule inhibitor of MET, on DMS273 small-cell lung cancer sublines. (a) Effect of PHA665752 on MET phosphorylation. G3H cells were starved in DMEM containing 0.5% FBS overnight, and then pre-incubated with PHA665752 (0.2 μM) for 2 h. Cells were then incubated with recombinant hepatocyte growth factor (HGF; 50 ng/mL) for 15 min. Cells were lysed immediately and whole cell lysate (20 μg) was analyzed by Western blotting. (b) *In vitro* sensitivity of the DMS273 sublines and MKN45 cell line against PHA665752. Cells were treated with the indicated concentrations of PHA665752 for 72 h. Assays were carried out in triplicate. The growth rate was calculated as the ratio of the MTT absorbance of PHA665752-treated cells compared with that of untreated cells. Results are expressed as means of three independent experiments ± SD. (c) Effect of PHA665752 and anti-HGF neutralizing antibodies on *in vitro* motility and invasion activities of G3H cells. *In vitro* motility and invasion assays using conditioned media of G3H as chemoattractant were carried out. Relative migrated or invaded cells were calculated as the ratio of numbers of migrated or invaded cells of the treated groups compared with the untreated group. Results are expressed as means of three independent experiments ± SD. *$P < 0.01$, **$P < 0.005$, Student's *t*-test, compared with untreated cells.

G3H, and PC-3 cells (Fig. 3d). These results suggest that DMS273-GFP and G3H cells were not MET-addicted, and that the HGF/MET signal was not essential for *in vitro* growth of these cells.

We then examined the effect of PHA665752 on *in vitro* motility and invasion activities in G3H cells. PHA665752 at 0.2 μM significantly suppressed both the motility and invasion activities of G3H cells when the CM of G3H cells, containing functional HGF (Fig. 3), was used as a chemoattractant (Fig. 4c). The magnitude of this suppression was the same using the anti-HGF neutralizing antibody as the HGF/MET signal blocker (Fig. 4c). These results indicated that HGF/MET is one of the important signal pathways for the *in vitro* motility and invasion activities of G3H cells and that PHA665752 has the ability to effectively inhibit these activities in G3H cells.

Based on our *in vitro* observations, we examined whether activation of the HGF/MET signal could be detected in tumors of our *in vivo* metastatic model. Immunohistological analysis showed that orthotopic tumors of G3H cells expressed HGF and MET and were positive for MET phosphorylation (pY1230/Y1234/Y1235) (Fig. 5a–e). These results support the notion of an autocrine HGF/MET signal in our model as observed in SCLC patients.

Next, we investigated the efficacy of pharmacological inhibition of the HGF/MET signal in our *in vivo* orthotopic metastatic model using G3H cells. Three days of treatment per week with PHA665752 at a dose of 15 mg/kg did not affect orthotopic tumor formation but decreased metastatic formations compared with vehicle treatment (distant metastases incidence, $P < 0.05$) (Fig. 5f,g). Additionally, we tested the *in*
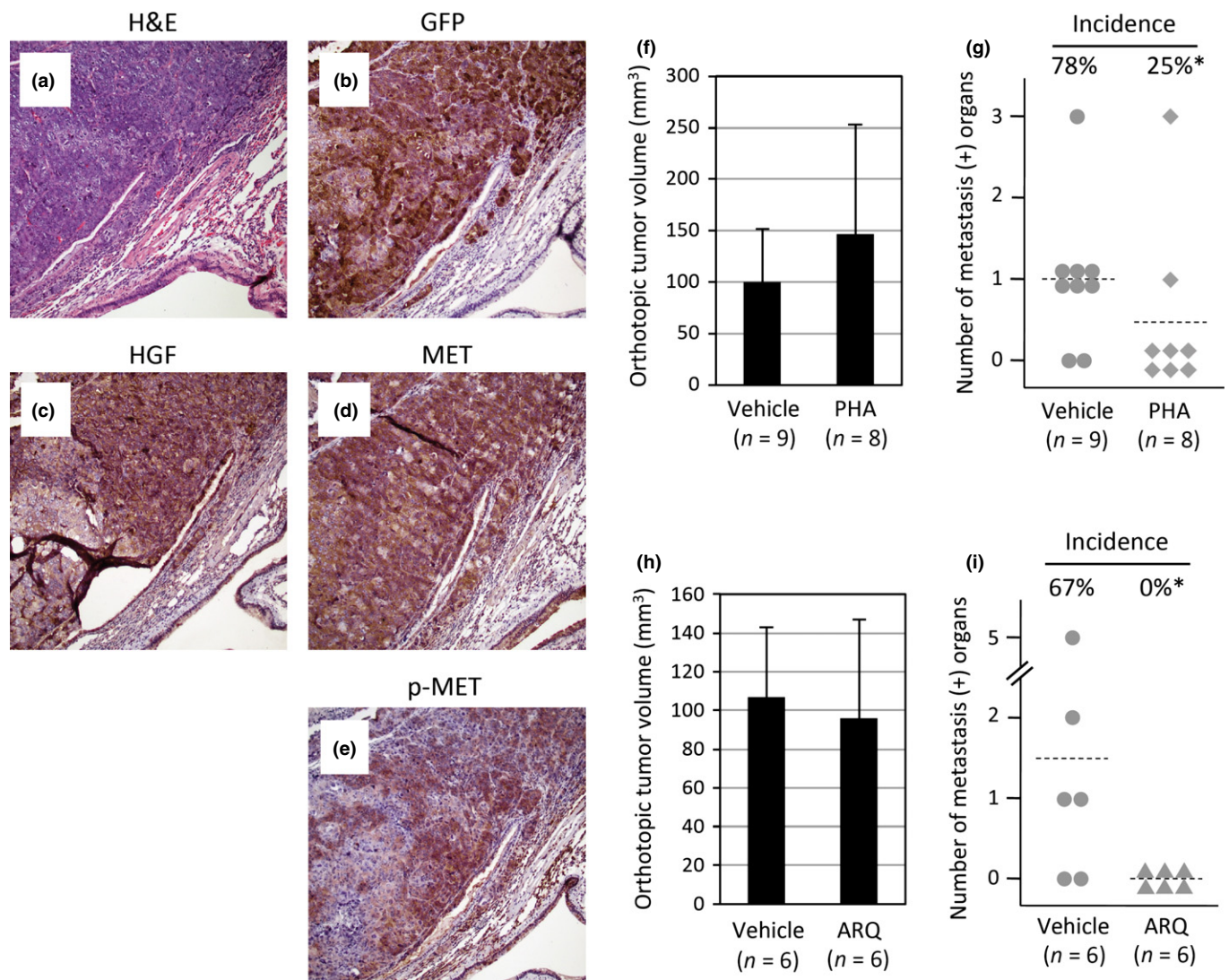

Fig. 5. Effect of MET inhibitors on orthotopic and metastatic tumor formation in our model of human small-cell lung cancer using G3H cells. (a–d) Immunostaining of hepatocyte growth factor (HGF)/MET in orthotopic tumors of our model using G3H cells. (a) H&E staining, (b) GFP immunostaining, (c) HGF immunostaining, (d) MET immunostaining, and (e) phosphorylation of MET (pY1230/Y1234/Y1235) immunostaining. (f, g) Effect of PHA665752 (PHA) treatment on orthotopic and metastatic tumor formation in our model using G3H cells. The mice were killed and assessed on day 27 or 28. (f) Orthotopic tumor formation. Results are expressed as means ± SD ($n = 8$ or 9). (g) Distant metastatic tumor formation. The dotted lines show the means of the number of metastasis-positive tissues of each group. Percentages show distant metastases incidence. *$P < 0.05$, Fisher's exact test. (h, i) Effect of ARQ-197 (ARQ) treatment on orthotopic and metastatic tumor formation in our model using G3H cells. The mice were killed and assessed on day 26. (h) Orthotopic tumor formation. Results are expressed as the means ± SD ($n = 6$). (i) Distant metastatic tumor formation. The dotted lines show the means of the number of metastasis-positive organs of each group. Percentages show distant metastases incidence. *$P < 0.05$, Fisher's exact test.

vivo effect of ARQ197, another MET inhibitor with microtubule inhibition activity.[19,20] ARQ197 treatment (120 mg/kg, 5 days/week) also did not affect the orthotopic tumor formation but decreased the metastatic formations more effectively than PHA665752 treatment (distant metastases incidence, $P < 0.05$) (Fig. 5h,i). Collectively, these data showed that the HGF/MET signal plays an important role in metastatic tumor formations in our model.

Discussion

We developed a new orthotopic model of SCLC metastasis using the GFP-labelled subline of the human SCLC cell line DMS273. In this model, metastases were detected in distant organs such as bone, kidney, and brain, similar to those observed in SCLC patients (Table 1).

Several studies have reported orthotopic SCLC models with metastatic potential. Onn *et al.*[21] reported an orthotopic model using the SCLC cell line NCI-H69. In this model, metastases to right lung and lymph node were observed. Daniel *et al.*[22] showed that metastases in mediastinal lymph node were detected in their model using cell lines derived from a primary xenograft model. Isobe *et al.*[23] developed three orthotopic SCLC models and detected micrometastasis in many distant organs, but not in the brain. Jacoby *et al.*[24] observed metastases to distant organs, including the brain, in a hypoxia-inducible factor-1α antagonist PX-478-treated group, but not in the drug-free group, in their model using the SCLC cell line NCI-H187. In our model, we detected macro- and micrometastases in the brain and other distant organs under drug-free conditions (Fig. 2, Table 1). Thus, distant metastases formation ability of our model is superior to that of other orthotopic SCLC models. DMS273 cells were established from cells in the pleural fluid of an SCLC patient and was classified as variant SCLC.[4,25] Variant SCLC cells had a faster growth rate and higher metastatic potential in an experimental metastatic model than classic SCLC cells.[3,26] These variant SCLC characteristics of DMS273 cells might be responsible for the aggressiveness of our model.

Many previous studies showed the importance of the HGF/MET signal in SCLC.[7–12] In this study, we found that the cells used in our model expressed both HGF and MET (Fig. 3), and that treatment with the MET inhibitor PHA665752 or anti-HGF neutralizing antibody significantly suppressed the *in vitro* migration and invasion activities of G3H cells using CM of G3H as a chemoattractant (Fig. 4). In addition, the more aggressive subline G3H derived from a bone metastasis showed higher HGF expression than the parental line (Fig. 3). We also detected HGF and MET expression *in vivo* and found that pharmacological inhibition of the HGF/MET signal suppressed distant metastases formation in our model using G3H cells (Fig. 5). These data collectively showed that the HGF/MET signal plays a pivotal role in our model, at least in part through the autocrine regulation as observed in SCLC patients. Hence, in addition to metastatic tropism, our model also mimics the pivotal signal pathway of clinical SCLC and can be used for the validation of HGF/MET target therapies for SCLC.

Obtaining clinical specimens of SCLC is difficult, as SCLC is not usually amenable to surgical management. This is one of the obstructions for identifying molecular mechanisms involved in the tumor progression and metastasis of SCLC. Our model has the same aspects of SCLC patients and the advantage of brain metastatic potential. Therefore, our orthotopic model of SCLC metastasis provides a new effective tool for the study of SCLC biology and development of novel SCLC treatments.

Disclosure Statement

The authors have no conflict of interest.

References

1 William WN Jr, Glisson BS. Novel strategies for the treatment of small-cell lung carcinoma. *Nat Rev Clin Oncol* 2011; **8**: 611–9.

2 Nicholson SA, Beasley MB, Brambilla E *et al.* Small cell lung carcinoma (SCLC): a clinicopathologic study of 100 cases with surgical specimens. *Am J Surg Pathol* 2002; **26**: 1184–97.

3 Carney DN, Gazdar AF, Bepler G *et al.* Establishment and identification of small cell lung cancer cell lines having classic and variant features. *Cancer Res* 1985; **45**: 2913–23.

4 Pedersen N, Mortensen S, Sørensen SB *et al.* Transcriptional gene expression profiling of small cell lung cancer cells. *Cancer Res* 2003; **63**: 1943–53.

5 Hann CL, Rudin CM. Fast, hungry and unstable: finding the Achilles' heel of small-cell lung cancer. *Trends Mol Med* 2007; **13**: 150–7.

6 Ghiso E, Giordano S. Targeting MET: why, where and how? *Curr Opin Pharmacol* 2013; **13**: 511–8.

7 Ma PC, Kijima T, Maulik G *et al.* MET mutational analysis in small cell lung cancer: novel juxtamembrane domain mutations regulating cytoskeletal functions. *Cancer Res* 2003; **63**: 6272–81.

8 Takigawa N, Segawa Y, Maeda Y, Takata I, Fujimoto N. Serum hepatocyte growth factor/scatter factor levels in small cell lung cancer patients. *Lung Cancer* 1997; **17**: 211–8.

9 Bharti A, Ma PC, Maulik G *et al.* Haptoglobin alpha-subunit and hepatocyte growth factor can potentially serve as serum tumor biomarkers in small cell lung cancer. *Anticancer Res* 2004; **24**: 1031–8.

10 Ma PC, Tretiakova MS, Nallasura V, Jagadeeswaran R, Husain AN, Salgia R. Downstream signalling and specific inhibition of MET/HGF pathway in small cell lung cancer: implication for tumor invasion. *Br J Cancer* 2007; **97**: 368–77.

11 Arriola E, Cañadas I, Arumí-Uría M *et al.* MET phosphorylation predicts poor outcome in small cell lung carcinoma and its inhibition blocks HGF-induced effects in MET mutant cell lines. *Br J Cancer* 2011; **105**: 814–23.

12 Maulik G, Kijima T, Ma PC *et al.* Modulation of the MET/hepatocyte growth factor pathway in small cell lung cancer. *Clin Cancer Res* 2002; **8**: 620–7.

13 Valastyan S, Weinberg RA. Tumor metastasis: molecular insights and evolving paradigms. *Cell* 2011; **147**: 275–92.

14 Price JE, Polyzos A, Zhang RD, Daniels LM. Tumorigenicity and metastasis of human breast carcinoma cell lines in nude mice. *Cancer Res* 1990; **50**: 717–21.

15 Hoffman RM. Orthotopic metastatic mouse models for anticancer drug discovery and evaluation: a bridge to the clinic. *Invest New Drugs* 1999; **17**: 343–59.

16 Dan S, Okamura M, Seki M *et al.* Correlating phosphatidylinositol 3-kinase inhibitor efficacy with signaling pathway status: in silico and biological evaluations. *Cancer Res* 2010; **70**: 4982–94.

17 Christensen JG, Schreck R, Burrows J *et al.* A selective small molecule inhibitor of MET kinase inhibits MET-dependent phenotypes in vitro and exhibits cytoreductive antitumor activity in vivo. *Cancer Res* 2003; **63**: 7345–55.

18 Smolen GA, Sordella R, Muir B *et al.* Amplification of MET may identify a subset of cancers with extreme sensitivity to the selective tyrosine kinase inhibitor PHA665752. *Proc Natl Acad Sci U S A* 2006; **103**: 2316–21.

19 Munshi N, Jeay S, Li Y *et al.* ARQ 197, a novel and selective inhibitor of the human c-Met receptor tyrosine kinase with antitumor activity. *Mol Cancer Ther* 2010; **9**: 1544–53.

20 Katayama R, Aoyama A, Yamori T *et al.* Cytotoxic activity of tivantinib (ARQ 197) is not due solely to c-MET inhibition. *Cancer Res* 2013; **73**: 3087–96.

21 Onn A, Isobe T, Itasaka S *et al.* Development of an orthotopic model to study the biology and therapy of primary human lung cancer in nude mice. *Clin Cancer Res* 2003; **9**: 5532–9.

22 Daniel VC, Marchionni L, Hierman JS *et al.* A primary xenograft model of small-cell lung cancer reveals irreversible changes in gene expression imposed by culture in vitro. *Cancer Res* 2009; **69**: 3364–73.

23 Isobe T, Onn A, Morgensztern D *et al.* Evaluation of novel orthotopic nude mouse models for human small-cell lung cancer. *J Thorac Oncol* 2013; **8**: 140–6.

24 Jacoby JJ, Erez B, Korshunova MV *et al.* Treatment with HIF-1alpha antagonist PX-478 inhibits progression and spread of orthotopic human small cell lung cancer and lung adenocarcinoma in mice. *J Thorac Oncol* 2010; **5**: 940–5.

25 Pettengill OS, Curphey TJ, Cate CC, Flint CF, Maurer LH, Sorenson GD. Animal model for small cell carcinoma of the lung: effect of immunosuppression and sex of mouse on tumor growth in nude athymic mice. *Exp Cell Biol* 1980; **48**: 279–97.

26 Shtivelman E, Namikawa R. Species-specific metastasis of human tumor cells in the severe combined immunodeficiency mouse engrafted with human tissue. *Proc Natl Acad Sci U S A* 1995; **92**: 4661–5.

Supporting Information

Additional supporting information may be found in the online version of this article:

Doc. S1. Materials and methods.

Fig. S1. Immunohistological analysis of orthotopic tumors and bone metastatic tumors of G3H cells.

Fig. S2. Immunohistological analysis of angiogenesis, lymphangiogenesis, and stromal reaction in orthotopic tumors of our orthotopic metastatic model.